Safe Screening for ℓ_2-norm Penalized Unbalanced Optimal Transport

Anonymous Author
Anonymous Institution

Abstract

HK comment: We change the story: (OT and UOT → Lasso-type UOT → Propose Screening (No literature) → Evaluation) The safe screening technique saves computational time by freezing the zero elements in the sparse solution of the Lasso problem. Recently, researchers have linked the UOT problem to the Lasso problem. In this paper, we propose a dynamic screening method to the ℓ_2-norm penalized unbalanced optimal transport (UOT) problem. We first apply the screening method to the UOT problem. We find out that the specific structure for the UOT problem allows it to get better screening results than the Lasso problem. We propose the new Dynamic Screening algorithm and demonstrate its extraordinary effectiveness and potential to benefit from the unique structure of the UOT problem, our algorithm substantially improves the screening efficiency compared to the standard Lasso Screening algorithm without significantly increasing the computational burden. We demonstrate the advantages of the algorithm through some experiments on the Gaussian distributions and the MNIST dataset.

1 INTRODUCTION

Optimal transport (OT) has a long history in mathematics and has recently become popular in machine learning and statistical learning due to its excellence in measuring the distance between two probability measures. It has outperformed traditional methods in many different areas such as domain adaptation

(Courty, 2017), generative models (Arjovsky et al., 2017), graph machine learning (Maretic et al., 2019) and natural language processing (Chen et al., 2019). The popularity of OT is attributed to the introduction of the Sinkhorn's algorithm (Sinkhorn, 1974) for the entropy-regularized Kantorovich formulation problem (Cuturi, 2013), which alleviates the computational burden in large-scale problems.

Addressing one limitation that the standard OT problem handles only *balanced* samples, the unbalanced optimal transport (UOT) has been proposed envisioning a wider range of applications with *unbalanced* samples (Caffarelli and McCann, 2010; Chizat et al., 2017). This application fields include, for example, computational biology (Schiebinger et al., 2019), machine learning (Janati et al., 2019) and deep learning (Yang and Uhler, 2019). Mathematically, UOT replaces the equality constraints with penalty functions on the marginal distributions with a divergence including KL divergence (Liero et al., 2018), and ℓ_1-norm (Caffarelli and McCann, 2010) and ℓ_2-norm distances (Benamou, Jean-David, 2003). The KL-penalized UOT with an entropy regularizer can be solved by the Sinkhorn algorithm (Pham et al., 2020). It is fast, scalable, and differentiable, but suffers from instability (Schmitzer, 2016), larger error, and a lack of sparsity in solution compared with other regularizers (Blondel et al., 2018). In contrast, ℓ_2-norm regularized UOT not only has a lower error but also brings a sparse solution. This attracted the attention of researchers to develop new and faster optimization algorithms (Blondel et al., 2018; Nguyen et al., 2022).

Despite the success in the development of fast and efficient optimization algorithms for UOT, the computational burden remains a bottleneck for large-scale applications. This paper tackles this issue from a different direction independent of optimization algorithms. Recently, Chapel et al. (2021) suggested a mutual connection between the UOT problem and the Lasso-like problem (Tibshirani, 1996; Efron et al., 2004) and the non-negative matrix factorization problem (Lee and Seung, 2000). This motivates us to adapt *safe screening* (Ghaoui et al., 2010) in these fields to accelerate

the computation of the UOT problem. In fact, the OT and UOT problems expect the solution to be sparse due to the effectiveness of their optimal transport cost and thus share a similar idea with the Lasso problem. Safe screening in the Lasso problem is a promising technique to speed up the computation by exploiting the sparsity of the solution. It eliminates elements in the solution that are guaranteed to be zero without solving the optimization problem. This does not affect the final solution. However, this straightforward application is not trivial, Since the cost matrix of the UOT problem has a wide range of values, the projection step in all Lasso screening method deteriorates when applied to the UOT problem, and fail as long as zero cost exists.

Specifically, while the Lasso problem has a dense *constraint matrix*, that of the UOT problem is extremely sparse and has a unique transport matrix structure. This would benefit the design of a specialized screening method and the outcome.

In this paper, we propose a new dynamic screening method designated to the UOT problem. To this end, we first derive a dual formulation of the vectorized Lasso-like UOT problem. Then, particularly addressing the structure of the constraint matrix, a dynamic screening method is derived, which includes a new projection method and a safe screening region construction method. These are suitable for the UOT problem and could largely improve the effects.

Contributions.:

- To the best of our knowledge, this work is the first dynamic screening method designated to the UOT problem, which is based on the Lasso-like formulation of the UOT problem and its dual formulation. Our proposed method is independent of optimization algorithms which could be combined will different solvers .

- We propose a projection method by leveraging the specific structure of the UOT problem, and it significantly reduces the errors in the projection process. We also propose a two hyper-plane method that can adjust the safe screening region for every primal element to achieve a better screening effect without adding computational burden.

- Numerical evaluation reveals their effectiveness in terms of projection distances and screening ratios compared with several methods including state-of-the-art methods.

The paper is organized as follows. **Section 2** presents preliminary descriptions of optimal transport and unbalanced optimal transport. The screening methods in Lasso-like problems are explained by addressing a dynamic screening framework. In **Section 3**, our proposed screening method for the UOT problem is detailed. **Section 4** shows numerical experiments.

2 PRELIMINARIES

$\mathbb{R}^n$ denotes n-dimensional Euclidean space, and $\mathbb{R}^n_+$ denotes the set of vectors in which all elements are non-negative. $\mathbb{R}^{m \times n}$ represents the set of $m \times n$ matrices. Also, $\mathbb{R}^{m \times n}_+$ stands for the set of $m \times n$ matrices in which all elements are non-negative. We present vectors as bold lower-case letters $\boldsymbol{a}, \boldsymbol{b}, \boldsymbol{c}, \dots$ and matrices as bold-face upper-case letters $\mathbf{A}, \mathbf{B}, \mathbf{C}, \dots$. The i-th element of $\boldsymbol{a}$ and the element at the (i, j) position of $\mathbf{A}$ are represented respectively as a_i and $A_{i,j}$. The i-th column of $\mathbf{A}$ is represented as $\boldsymbol{a}_i$. In addition, $\mathbb{1}_n \in \mathbb{R}^n$ is the n-dimensional vector in which all the elements are one. For $\boldsymbol{x}$ and $\boldsymbol{y}$ of the same size, $\langle \boldsymbol{x}, \boldsymbol{y} \rangle = \boldsymbol{x}^T \boldsymbol{y}$ is the Euclidean dot-product between vectors. For two matrices of the same size $\mathbf{A}$ and $\mathbf{B}$, $\langle \mathbf{A}, \mathbf{B} \rangle = \text{tr}(\mathbf{A}^T \mathbf{B})$ is the Frobenius dot-product. We use $\|\boldsymbol{a}\|_2$ and $\|\boldsymbol{a}\|_1$ to represent the ℓ_2-norm and ℓ_1-norm of $\boldsymbol{a}$, respectively. D_ϕ is the Bregman divergence with the strictly convex and differentiable function ϕ, i.e., $D_\phi(\boldsymbol{a}, \boldsymbol{b}) = \sum_i d_\phi(a_i, b_i) = \sum_i [\phi(a_i) - \phi(b_i) - \phi'(a_i)(a_i - b_i)]$. In addition, we suggests a vectorization for $\mathbf{A} \in \mathbb{R}^{m \times n}$ as a lowercase letters $\boldsymbol{a} \in \mathbb{R}^{mn}$ and $\boldsymbol{a} = \text{vec}(\mathbf{A}) = [\mathbf{A}_{1,1}, \mathbf{A}_{1,2}, \cdots, \mathbf{A}_{m,n-1}, \mathbf{A}_{m,n}]$.

2.1 Optimal Transport and Unbalanced Optimal Transport

Optimal Transport (OT): Given two discrete probability measures $\boldsymbol{a} \in \mathbb{R}^m$ and $\boldsymbol{b} \in \mathbb{R}^n$, the standard OT problem seeks a corresponding *transport matrix* $\mathbf{T} \in \mathbb{R}^{m \times n}_+$ that minimizes the total transport cost (Kantorovich, 1942). This is a linear programming problem formulated as

$$\text{OT}(\boldsymbol{a}, \boldsymbol{b}) \quad := \quad \min_{\mathbf{T} \in \mathbb{R}^{m \times n}_+} \langle \mathbf{C}, \mathbf{T} \rangle \qquad (1)$$
$$\text{subject to} \qquad \mathbf{T} \mathbb{1}_n = \boldsymbol{a}, \mathbf{T}^T \mathbb{1}_m = \boldsymbol{b},$$

where $\mathbf{C} \in \mathbb{R}_+{}^{m \times n}$ is the *cost matrix*. The constraints in (1) are so-called *mass-conservation constraints* or *marginal constraints*, and assume $\|\boldsymbol{a}\|_1 = \|\boldsymbol{b}\|_1$. Thus, the solution $\hat{\boldsymbol{t}}$ does not exist when $\|\boldsymbol{a}\|_1 \neq \|\boldsymbol{b}\|_1$. The obtained OT matrix $\mathbf{T}^*$ brings powerful distances as $\mathcal{W}_p = \langle \mathbf{T}^*, \mathbf{C} \rangle^{\frac{1}{p}}$, which is known as the p-th order *Wasserstein distance* (Villani, 2008).

As $\boldsymbol{t} = \text{vec}(\mathbf{T}) \in \mathbb{R}^{mn}$ and $\boldsymbol{c} = \text{vec}(\mathbf{C}) \in \mathbb{R}^{mn}$, we reformulate Eq.(1) in a vector format as (Chapel et al.,

2021)

$$\begin{aligned} \text{OT}(\boldsymbol{a}, \boldsymbol{b}) \quad &:= \quad \min_{\boldsymbol{t} \in \mathbb{R}_+^{mn}} \boldsymbol{c}^T \boldsymbol{t} \qquad\qquad (2) \\ \text{subject to} \quad &\qquad \mathbf{N}\boldsymbol{t} = \boldsymbol{a}, \mathbf{M}\boldsymbol{t} = \boldsymbol{b}, \end{aligned}$$

where $\mathbf{N} \in \mathbb{R}^{m \times mn}$ and $\mathbf{M} \in \mathbb{R}^{n \times mn}$ are two matrices composed of "0" and "1". $\mathbf{N}$ and $\mathbf{M}$ in case of $m = n = 3$ are given, respectively, as

$$\mathbf{N} = \begin{pmatrix} 1 & 1 & 1 & 0 & 0 & 0 & 0 & 0 & 0 \\ 0 & 0 & 0 & 1 & 1 & 1 & 0 & 0 & 0 \\ 0 & 0 & 0 & 0 & 0 & 0 & 1 & 1 & 1 \end{pmatrix},$$

$$\mathbf{M} = \begin{pmatrix} 1 & 0 & 0 & 1 & 0 & 0 & 1 & 0 & 0 \\ 0 & 1 & 0 & 0 & 1 & 0 & 0 & 1 & 0 \\ 0 & 0 & 1 & 0 & 0 & 1 & 0 & 0 & 1 \end{pmatrix}.$$

Note that $\mathbf{N}$ and $\mathbf{M}$ both have a specific structure, where each column has only one single non-zero element equal to 1.

Unbalanced Optimal Transport (UOT): The marginal constraints in (1) may exacerbate degradation of the performance of some applications where weights need not be strictly preserved. In contrast, the UOT problem *relaxes* them by replacing the equality constraints with penalty functions on the marginal distributions with a divergence. Formally, defining $\boldsymbol{y} = [\boldsymbol{a}, \boldsymbol{b}]^T \in \mathbb{R}^{mn}$ and $\mathbf{X} = [\mathbf{M}^T, \mathbf{N}^T]^T \in \mathbb{R}^{(m+n) \times mn}$, the UOT problem can be formulated introducing a penalty function for the histograms as (Chapel et al., 2021)

$$\text{UOT}(\boldsymbol{a}, \boldsymbol{b}) := \min_{\boldsymbol{t} \in \mathbb{R}_+^{mn}} \boldsymbol{c}^T \boldsymbol{t} + D_\phi(\mathbf{X}\boldsymbol{t}, \boldsymbol{y}). \qquad (3)$$

It is worth mentioning that this function is convex due to the convexity of the Bregman divergence.

Relationship with Lasso-like problem: The Lasso-like problem has a general formula:

$$f(\boldsymbol{t}) \quad := \quad g(\boldsymbol{t}) + D_\phi(\mathbf{X}\boldsymbol{t}, \boldsymbol{y}).$$

Substituting $g(\boldsymbol{t}) = \lambda\|\boldsymbol{t}\|_1$ $(\lambda > 0)$ and $D_\phi(\mathbf{X}\boldsymbol{t}, \boldsymbol{y}) = \frac{1}{2}\|\mathbf{X}\boldsymbol{t} - \boldsymbol{y}\|_2^2$ into $f(\boldsymbol{t})$ above reduces to the standard ℓ_2-norm regularized Lasso problem. On the other hand, addressing that $\boldsymbol{c}$ and $\boldsymbol{t}$ in (3) are nonnegative, the term $\boldsymbol{c}^T \boldsymbol{t}$ is represented as $\boldsymbol{c}^T \boldsymbol{t} = \sum_i c_i t_i = \sum_i c_i|t_i|$. Therefore, the UOT problem in (3) is equivalent to a weighted ℓ_1-norm regularized Lasso-like problem. It is, however, that $\mathbf{X} = [\mathbf{M}^T, \mathbf{N}^T]^T$ in (3) substantially differs from that of the Lasso problem. More concretely, the former $\mathbf{X}$ has a specific structure and has only two non-zero elements equal to 1 in each row whereas the latter $\mathbf{X}$ in Lasso problem is non-structured and dense (Chapel et al., 2021).

2.2 Dynamic Screening Framework

Solutions to many large-scale optimization problems tend to be sparse, and a large amount of computation is wasted on updating the zero elements during the optimization process. Screening technique is a well-known technique in the Lasso problem and the SVM problem (Ogawa et al., 2013), where the ℓ_1-norm regularizer leads to a sparse solution for the problem (Ghaoui et al., 2010). It can pre-select solutions that must be zero theoretically and freeze them before optimization computation, thus saving optimization time. Many safe screening methods have been proposed in this past decade (Liu et al., 2014; Wang et al., 2015), and recent dynamic screening methods efficiently drop variable elements, which include Dynamic Screening (Bonnefoy et al., 2015), Gap Safe screening (Ndiaye et al., 2017) and Dynamic Sasvi (Yamada and Yamada, 2021).

Hereinafter, we briefly elaborate on the framework proposed in (Yamada and Yamada, 2021) to introduce the whole dynamic screening technique for the Lasso-like problem:

$$\min_{\boldsymbol{t}} \{f(\boldsymbol{t}) := g(\boldsymbol{t}) + h(\mathbf{X}\boldsymbol{t})\}. \qquad (4)$$

The Fenchel-Rockafellar Duality yields the dual problem as presented below:

Theorem 1 (Fenchel-Rockafellar Duality (Rockafellar and Wets, 1998))**.** *If h and g are proper convex functions on $\mathbb{R}^{m+n}$ and $\mathbb{R}^{mn}$. Then we have the following:*

$$\min_{\boldsymbol{t}} g(\boldsymbol{t}) + h(\mathbf{X}\boldsymbol{t}) = \max_{\boldsymbol{\theta}} -h^*(-\boldsymbol{\theta}) - g^*(\mathbf{X}^T\boldsymbol{\theta}). \quad (5)$$

Because the primal function h is always convex, the dual function h^* is concave. Assuming h^* is an L-strongly concave problem, we can design an area for any feasible $\tilde{\boldsymbol{\theta}}$ by the strongly concave property:

Theorem 2 (L-strongly concave (Yamada and Yamada, 2021, Theorem 5))**.** *Considering problem in Eq.(4), if function h and g are both convex, for $\forall \ \tilde{\boldsymbol{\theta}}$ and satisfied the constraints on the dual problem, we have the following area constructed by its L-strongly concave property:*

$$\mathcal{R} := \boldsymbol{\theta} \in \left\{ \frac{L}{2}\|\boldsymbol{\theta} - \tilde{\boldsymbol{\theta}}\|_2^2 + h^*(-\tilde{\boldsymbol{\theta}}) \leq h^*(-\boldsymbol{\theta}) \right\}.$$

Theorem 3 (Circle constraint for Lasso-like problem (Yamada and Yamada, 2021, Theorem 8))**.** *Consider the Lasso-like problem and Fenchel-Rockafellar Duality by Eq.(5). We assume that $\tilde{\boldsymbol{\theta}}$ is inside the domain of the dual problem. Then, $\mathcal{R}$ in **Theorem 2** is equivalent to the following circle constraint $\mathcal{R}^C$:*

$$\mathcal{R}^C := \{\boldsymbol{\theta} \mid (\boldsymbol{\theta} - \tilde{\boldsymbol{\theta}})^T(\boldsymbol{\theta} - \boldsymbol{y}) \leq 0\}. \qquad (6)$$

$\boldsymbol{\theta}$ and $\boldsymbol{y}$ are the endpoints of the diameter of this circle, and $\hat{\boldsymbol{\theta}} \in \mathcal{R}^C$.

As the dual optimal solution $\hat{\boldsymbol{\theta}}$ satisfies the **Theorem 2** as a corollary of L-strongly concave property. The area $\mathcal{R}^C$ is not empty.

3 PROPOSED UOT SCREENING

This section proposes a new safe screening region $\mathcal{R}^S$ for the UOT problem, and a projection method to perform our dynamic screening based on $\mathcal{R}^S$. $\mathcal{R}^S$ is composed of the circle constraint $\mathcal{R}^C$ in **Theorem 3** and the relaxed region of the dual feasible area $\mathcal{R}^D$. After deriving the dual formulation of the Lasso-like formulated UOT problem in Eq.(3) and $\mathcal{R}^D$, we derive $\mathcal{R}^S$ by relaxing $\mathcal{R}^D$. Concrete proofs of lemma and theorems are provided in the supplementary file.

3.1 Safe Region Construction

Dual formulation of UOT: The UOT problem has the form of $h(\mathbf{X}t) = \frac{1}{2}\|\mathbf{X}t - \boldsymbol{y}\|_2^2$ and $g(\boldsymbol{\theta}) = \lambda \boldsymbol{c}^T \boldsymbol{t}$, where $t_i \geq 0$ for $i \in [mn]$ in Eq.(4). Also, $\boldsymbol{\theta} = [\boldsymbol{\alpha}^T, \boldsymbol{\beta}^T]^T \in \mathbb{R}^{m+n}$, where $\boldsymbol{\alpha} \in \mathbb{R}^m$ and $\boldsymbol{\beta} \in \mathbb{R}^n$. We obtain the dual form by **Theorem 1**:

Lemma 4 (Dual form of the UOT problem). *For the UOT problem in Eq.(3), we obtain the following dual problem:*

$$-h^*(-\boldsymbol{\theta}) - g^*(\mathbf{X}^T\boldsymbol{\theta}) = -\frac{1}{2}\|\boldsymbol{\theta}\|_2^2 + \boldsymbol{y}^T\boldsymbol{\theta} \quad (7)$$
$$\text{subject to} \quad \boldsymbol{x}_p^T\boldsymbol{\theta} - \lambda c_p \leq 0, \quad \forall p \in [mn],$$

where $\boldsymbol{x}_p$ corresponds to the p-th column of $\mathbf{X}$.

The strongly concave coefficient L for the dual function f is 1.

Dual feasible region $\mathcal{R}^D$: The constraint in Eq.(7) specifies a dual variable feasible area, denoted as $\mathcal{R}^D$, and the optimal dual solution $\hat{\boldsymbol{\theta}} \in \mathcal{R}^D$ because of **Theorem 2**.

According to the the KKT condition of the Fenchel-Rockafellar Duality in **Theorem 1**, there is a connection between the optimal primal and dual solutions $\hat{\boldsymbol{t}}$ and $\hat{\boldsymbol{\theta}}$ that:

Theorem 5. *(From the KKT condition) For the primal optimal solution $\hat{\boldsymbol{t}}$ and the dual optimal solution $\hat{\boldsymbol{\theta}}$, we have the following relationship:*

$$\boldsymbol{x}_p^T\hat{\boldsymbol{\theta}} - \lambda c_p \begin{cases} < 0 & \implies & \hat{t}_p = 0 \\ = 0 & \implies & \hat{t}_p \geq 0. \end{cases} \quad (8)$$

The proof of **Theorem 5** is given in the Appendix. Eq.(8) indicates a potential method to screen the primal variable $\boldsymbol{t}$. However, since we do not know the

optimal dual solution $\hat{\boldsymbol{\theta}}$ directly, this paper seeks a safe screening region for sceening, denoted as $\mathcal{R}^S$, as small as possible that contains the $\hat{\boldsymbol{t}}$. In other words, if

$$\max_{\boldsymbol{\theta} \in \mathcal{R}^S} \quad \boldsymbol{x}_p^T\boldsymbol{\theta} - \lambda c_p < 0. \quad (9)$$

then we assert $\boldsymbol{x}_p^T\hat{\boldsymbol{\theta}} - \lambda c_p < 0$, which means the corresponding $\hat{t}_p = 0$, and can be screened out.

For this purpose, we focus on the special structure of $\mathbf{X}$ in the UOT problem, i.e., the p-th column of $\mathbf{X}$ has only two nonzero elements equal to 1. Defining $\boldsymbol{\theta} = [\boldsymbol{\alpha}^T, \boldsymbol{\beta}^T]^T$, and $(u, v) = (p \mid n, v = p \mod n)$, we rewrite $\boldsymbol{x}_p^T\hat{\boldsymbol{\theta}} - \lambda c_p < 0$ as

$$\alpha_u + \beta_v - \lambda c_p < 0. \quad (10)$$

The nm inequalities can be reorgnized as a $m \times n$ matrix like Fig. 1, every elements of the matrix is an inequality If we obtain $\tilde{\boldsymbol{\theta}}$ in $\mathcal{R}^D$, combining $\mathcal{R}^D$ with $\mathcal{R}^C$ in **Theorem 3**, we can use $\mathcal{R}^C \cap \mathcal{R}^D$ as the area $\mathcal{R}^S$ in Eq.(9). The problems' difficulties are (i) maximizing on the $\mathcal{R}^D$ is time consuming, and (ii) we need a $\tilde{\boldsymbol{\theta}} \in \mathcal{R}^D$ first to construct the $\mathcal{R}^{\mathcal{C}}$. We address two issues below:

Relaxed feasible region $\mathcal{R}^D$ and safe screening region $\mathcal{R}^S$: As $\mathcal{R}^D$ is a $(n + m)$-polytope with nm Facets, it is time-consuming to maximize one time on the intersection of a hyper-ball and a polytope with simplex or Lagrange method not that than for every primal element t_p

The most direct method for dealing with the problem is to *relax* the polytope constraint into a hyper-plane constraint. Thus, considering the specific structure of the $\mathbf{X}$ in the UOT problem, our proposed method relaxes the polytope into two planes by combining the nm dual constraints with a positive weight $t_p \geq 0$, not like (Xiang et al., 2017), we can design 2 specific planes for every single element in the UOT problem and maximizing on them without adding extra computational burden. If the constraint is relevant to the dual elements α_u and β_v, which would largely influence the screening of t_p, we add it to the group 1, and the rest of constraints are added to the group 2. More concretely, we divide the polytope constraints into two groups I_p and I_p^C for every p, two-planes area are $\mathcal{R}_p^S$ is smaller than the relaxation in (Yamada and Yamada, 2021), Moreover, benefiting from the structure of $\boldsymbol{x}_p^T\boldsymbol{\theta} = \alpha_v + \beta_v$, we can put $m + n$ constraints that are directly connected with the optimization direction together, to alleviate the relaxation influence caused by the secondary dual variables.

Theorem 6 (Cruciform Two-plane safe screening region for UOT). *For every primal variable $\boldsymbol{t}$, $t_l \geq 0$, $l \in [mn]$, let $I_p = \{i \mid 0 \leq i < nm, u = i \mid n \lor v = i$

mod $n\}$, and $I_p^C = \{i \mid 0 \leq i < nm, i \notin I_p\}$. *Then, we construct a specific area $\mathcal{R}_p^S$ as presented below:*

$$\mathcal{R}_p^S(\boldsymbol{\theta}, \boldsymbol{t}) := \left\{ \boldsymbol{\theta} \middle| \begin{array}{l} \sum_{l \in I_p}(\boldsymbol{x}_l^T\boldsymbol{\theta} - \lambda c_l)t_l \leq 0, \\ \sum_{l \in I_p^C}(\boldsymbol{x}_l^T\boldsymbol{\theta} - \lambda c_l)t_l \leq 0, \\ (\boldsymbol{\theta} - \tilde{\boldsymbol{\theta}})^T(\boldsymbol{\theta} - \boldsymbol{y}) \leq 0 \end{array} \right\}. \quad (11)$$

Consequently, we have $\hat{\boldsymbol{\theta}} \in \mathcal{R}^C \cap \mathcal{R}^D \subset \mathcal{R}_p^S$ (The proof is given in the Appendix). We designate this as *cruciform two-plane screening (CTP)* in this paper. As $\mathcal{R}^C$ is a circle, we assume its center is θ_o, then we rewrite $\boldsymbol{\theta} = \boldsymbol{\theta}_o + \boldsymbol{q}$, $r = \frac{\|\boldsymbol{y} - \boldsymbol{\theta}\|_2}{2}$, the Lagrange function of the optimization problem is

$$\min_{\boldsymbol{q}} \max_{\eta,\mu,\nu \geq 0} L(\boldsymbol{q}, \eta, \mu, \nu) = \min_{\boldsymbol{q}} \max_{\eta,\mu,\nu \geq 0} -\boldsymbol{x}_p^T\boldsymbol{\theta}_o$$
$$- \boldsymbol{q}_u - \boldsymbol{q}_{u+v+1} + \eta(\boldsymbol{q}^T\boldsymbol{q} - r^2)$$
$$+ \mu((\sum_{l \in I_p} \boldsymbol{x}_l)^T(\boldsymbol{q} + \boldsymbol{\theta}_o) - \lambda \sum_{l \in I_p} c_l t_l)) \quad (12)$$
$$+ \nu((\sum_{l \in I_p^C} \boldsymbol{x}_l)^T(\boldsymbol{q} + \boldsymbol{\theta}_o) - \lambda \sum_{l \in I_p^C} c_l t_l)$$

This problem can be solved easily by the Lagrangian method in constant time. Its computational process is detailed in the supplementary material. A.

3.2 Projection Method

Before we start to screening with the safe screening region $\mathcal{R}^S$ that is constructed by **Theorem 6**, we first have to find a dual variable $\tilde{\boldsymbol{\theta}} \in \mathcal{R}^D$. Although there exists a relationship between the primal variable and dual variable that $\boldsymbol{\theta} = \boldsymbol{y} - \mathbf{X}\boldsymbol{t}$, inevitably, we often get $\boldsymbol{\theta} \notin \mathcal{R}^D$. This requires us to project $\boldsymbol{\theta}$ onto $\mathcal{R}^D$. Dynamic screening gets a more accurate screening outcome because the optimization algorithm gradually provides $\boldsymbol{t}^k \to \hat{\boldsymbol{t}}$, and also the dual variable $\boldsymbol{\theta}^k \to \hat{\boldsymbol{\theta}}$. If $\tilde{\boldsymbol{\theta}} \to \hat{\boldsymbol{\theta}}$, the safe screening region $\mathcal{R}^C \cap \mathcal{R}^D$ would get smaller and has a better screening outcome. As $\mathcal{R}^D$ is a polytope combined with nm hyperplanes, the cost of a real projection is expensive whether you choose Linear programming or Dykstra's projection algorithm. To this issue, in the Standard Lasso problem, the dual constraints in Eq.(7) is $\|\boldsymbol{x}_p\hat{\boldsymbol{\theta}}\|_1 \leq \lambda$, where $\boldsymbol{x}_p$ is almost dense and non-structured, researchers always uses a simple shrinking method to obtain a $\tilde{\boldsymbol{\theta}} \in \mathcal{R}^D$ as $\tilde{\boldsymbol{\theta}} = \frac{\boldsymbol{\theta}}{\max(1, \|\mathbf{X}^T\boldsymbol{\theta}/\lambda\|_\infty)}$ (Ndiaye et al., 2017, Proposition 11) (Yamada and Yamada, 2021, Theorem 11).

One straightforward extension of this into the UOT problem could be

$$\tilde{\boldsymbol{\theta}} = \frac{\boldsymbol{\theta}}{\max(1, \|\frac{\mathbf{X}^T\boldsymbol{\theta}}{\lambda\boldsymbol{c}^T}\|_\infty)},$$

where $(\stackrel{.}{\div})$ is the element-wise division. However, this projection pushes $\boldsymbol{\theta}$ far away from the optimal solution $\hat{\boldsymbol{\theta}}$ because it suffers from the influence of a small c_p. Also, it will degenerate when one of the costs is $c_p = 0$, and disables the screening process. Therefore, noting that the UOT problem, only allows $t_p \geq 0$, and the $\boldsymbol{x}_p$ only consists of two non-zero elements, we can adapt a better and cheap projection method. Specifically, we shift every single α_u, β_v with half of the maximum differences in all of its constraints.

The following theorem states this:

Theorem 7 (UOT shifting projection). *For any $\boldsymbol{\theta} = [\boldsymbol{\alpha}^T, \boldsymbol{\beta}^T]^T$, we define the projection operator $\tilde{\boldsymbol{\theta}} = $ Projection$(\boldsymbol{\theta})$, where*

$$\tilde{\alpha}_u = \alpha_u - \max_{0 \leq j < n} \frac{\alpha_u + \beta_j - \lambda c_{un+j}}{2}$$
$$\tilde{\beta}_v = \beta_v - \max_{0 \leq i < m} \frac{\alpha_i + \beta_v - \lambda c_{in+v}}{2} \quad (13)$$

$$(14)$$

Then, the calculated $\tilde{\boldsymbol{\theta}} = [\tilde{\boldsymbol{\alpha}}^T, \tilde{\boldsymbol{\beta}}^T]^T \in \mathcal{R}^D$.

The proof is in the supplementary material. Note that this cheap projection method can get good accuracy with $O(knm)$ computational time.
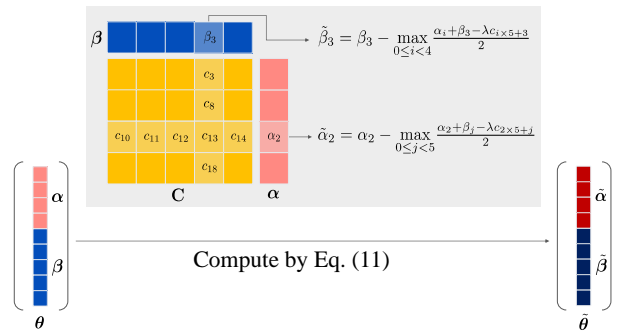

Figure 1: Example of Shifting Projection on a 4×5 matrix.

3.3 Screening Algorithms

The purpose of screening methods is to remove variable elements that are ignored at the optimization process in the adopted optimization algorithm. For this, we denote $\boldsymbol{s} \in \mathbb{R}^{mn}$ as the *screening mask vector* for the transport vector $\boldsymbol{t}$. Thus, $s_p = 0$ implies that the
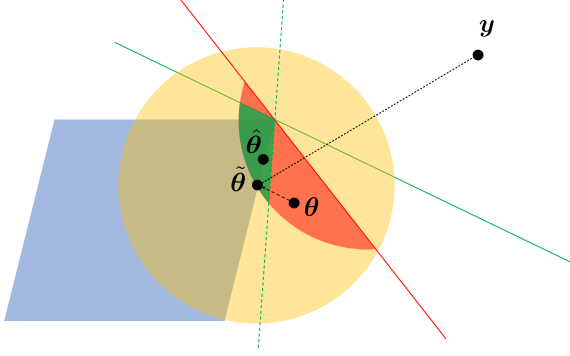
Figure 2: Comparision of Gap region (yellow), Dynamic Sasvi's region (red) and CTP method's region (green), the blue part is the $\mathcal{R}^D$

Algorithm 1 UOT Optimization with Dynamic Screening

Input: $\boldsymbol{t}_0, \boldsymbol{s} \in \mathbb{R}^{nm}, s_p = 1 \; \forall p \in [mn], w$
Output: $\boldsymbol{t}^K$
    for $k = 0$ to $K - 1$ **do**
        if $k \mod w = 0$ **then**
            $\tilde{\boldsymbol{\theta}}^k = \text{Projection}(\boldsymbol{\theta}^k)$ Eq.(14)
            for $p = 0$ to $mn - 1$ **do**
                $\mathcal{R}^S \leftarrow \mathcal{R}^S_p(\tilde{\boldsymbol{\theta}}^k, \boldsymbol{t}^k)$ Eq.(11)
                $\boldsymbol{s} \leftarrow s_p = 0$ if $\max\limits_{\boldsymbol{\theta} \in \mathcal{R}^S} \boldsymbol{x}_p{}^T \boldsymbol{\theta}^k < \lambda c_p$ Eq.(9)
            end for
        end if
        $\boldsymbol{t}^{k+1} = \text{update}(\boldsymbol{t}^k, \boldsymbol{s})$ (Optimization process)
    end for
    return $\boldsymbol{t}^K$

---

corresponding t_p should be screened out. We summarize a specific algorithm for ℓ_2-norm penalized UOT problem to show the entire optimization process as in **Algorithm 1**. The update$(\boldsymbol{t}, \boldsymbol{s})$ operator in the algorithm indicates the updating process for $\boldsymbol{t}$ by using an adopted optimizer, the optimizer would ignore the variables t_p that has been screened out that $s_p = 0$. $rw \in \mathbb{N}$ specifies the period of the screening to update the mask $\boldsymbol{s}$, because the change in screening ratio is acturally small if we update $\boldsymbol{s}$ every time. The period w is decided by a user, and the faster converging the optimizer is, the smaller period r is. It should be emphasized that the proposed screening method is *independent* of the adopted optimization algorithm.

3.4 Computational Cost Analysis

Our proposed method needs to construct different plans for every single primal element p, however, thanks to the special structure of the $\mathbf{X}$, For every single t_p, the data required for maximizing (by Lagrange method in supplementary material) can be summa-

rized as some specific sum, which can be computed together and reuse for other elements have the same $t \mod m$ or $t \mid m$. It helps us to preserve the whole optimization complexity to $O(kmn)$, k is a constant.

4 EXPERIMENTS

In this section, we organize some experiments on randomly generated gaussian distributions and MNIST dataset. We proved the projection effectiveness of our method by measuring the distance between the dual variable and the projected point. We compared our proposed Two-plane Dynamic Screening with some state-of-the-art methods. We also applied our Screening method on some famous l_2 norm UOT problem solvers like FISTA, BFGS, Lasso (celer), Multiplicative update, and Regularization path to test its speed-up ratio.

4.1 Projection Method

To prove the effectiveness of our projection method compared with the traditional projection method in the Lasso problem, we compared the projection distance and screening ratio with randomly generated Gaussian measures by two projection methods. We set the $\lambda = \frac{\|\mathbf{X}^T y\|}{100}$ and test for 10 different pairs. We choose the FISTA for solving the L_2 penalized UOT problems. Because the standard Lasso projection method would degenerate when $c_p = 0$, we add a small constant $\epsilon = 0.01$ on the cost matrix for both methods. Our projection method has only moved the dual point a little to ensure it is inside the $\mathcal{R}^D$ the order of magnitude is ignorable. It ensures the projection step would not harm the approximation process for the computational dual solution $\boldsymbol{\theta}^k$ to the optimum $\hat{\theta}$.

4.2 Comparing with Other Screening Methods

We compared the proposed screening ratio with three different methods, including our Cross Two-Plane method (CTP), a Random Two-Plane method (RTP), Dynamic Sasvi method, and Gap method. All the methods would use our projection method as it has been proven better than the standard Lasso projection method. It is clear that the CTP still outperform all the other method, CTP can start screening at a very early stage. The RTP just randomly divides the constraints and combines them into two planes, Although RTP is still better than the Sasvi algorithm, the performance is worse than CTP. which indicates that our achievements should not be simply attributed to the choice of more planes, The effectiveness is highly con-
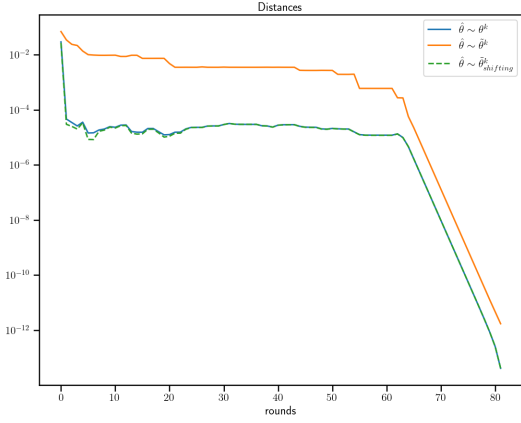
Figure 3: Distance of different projection method
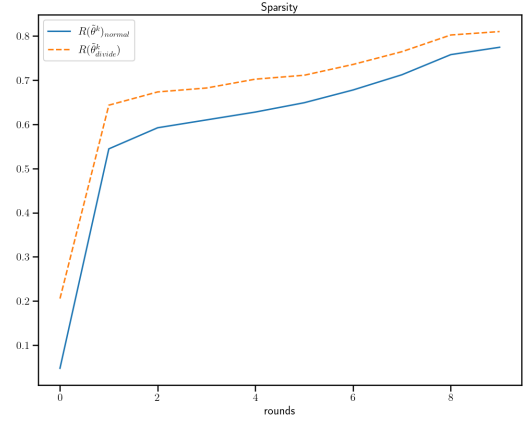

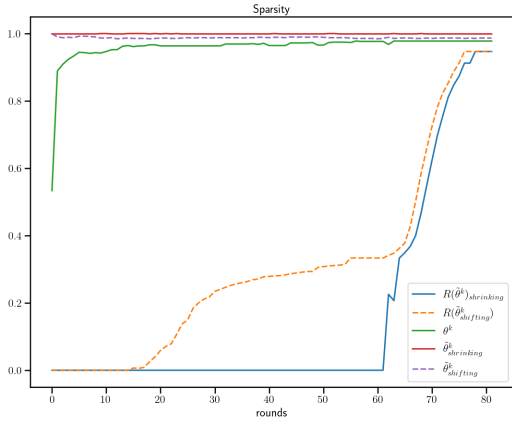Figure 5: Screening ratio of dividing method

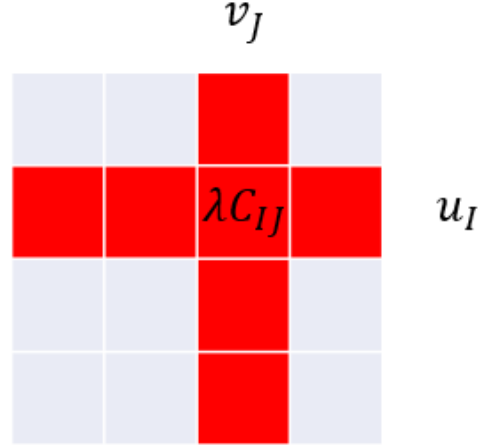Figure 4: Screening ratio of different projection method

Figure 6: speed up ratio for different solver

nected with the specific structure of the UOT problem, which decrease the influence of other variables and make us able to divide the constraints according to the variables.

4.3 Speed up Ratio

We applied the CTP in different UOT optimizers like FISTA, BFGS, Lasso(celer), Multiplicative update, and Regularization path method, and use them to solve the UOT problem between random number figure pairs in the MNIST dataset, we compared the consuming time for different accuracy and showed in the table, Our Screening method can get a good speed up ratio for almost every optimizer, and performs especially good on Multiplicative update algorithms

5 CONCLUSION

This paper introduced the Screening method in the Lasso community to the UOT problem and demonstrates that the screening method has extra potential to make a difference in the UOT community due to its specific structure. We provide a better projection method for the UOT screening process and design a Cross Two-Plane safe Screening region for it, which accomplishes a good performance and shows the potential to exploit the structure of the UOT problem. We believe these approaches can be extended to other regularized and penalized UOT problems like KL penalized UOT (Dantas et al., 2021) problem and even entropic UOT problem. we are going to combine our method with the Sinkhorn algorithm to alleviate its

drawbacks on computational time and sparsity.

References

Arjovsky, M., Chintala, S., and Bottou, L. (2017). Wasserstein generative adversarial networks. In *ICML*.

Benamou, Jean-David (2003). Numerical resolution of an "unbalanced" mass transport problem. *ESAIM: M2AN*, 37(5):851–868.

Blondel, M., Seguy, V., and Rolet, A. (2018). Smooth and sparse optimal transport. In *AISTATS*.

Bonnefoy, A., Emiya, V., Ralaivola, L., and Gribonval, R. (2015). Dynamic screening: Accelerating first-order algorithms for the lasso and group-lasso. *IEEE Transactions on Signal Processing*, 63(19):5121–5132.

Caffarelli, L. A. and McCann, R. J. (2010). Free boundaries in optimal transport and Monge-Ampère obstacle problems. *Annals of Mathematics*, 171(2):673–730.

Chapel, L., Flamary, R., Wu, H., Févotte, C., and Gasso, G. (2021). Unbalanced optimal transport through non-negative penalized linear regression. In *NeurIPS*.

Chen, L., Zhang, Y., Zhang, R., Tao, C., Gan, Z., Zhang, H., Li, B., Shen, D., Chen, C., and Carin, L. (2019). Improving sequence-to-sequence learning via optimal transport. In *ICLR*.

Chizat, L., Peyré, G., Schmitzer, B., and Vialard, F.-X. (2017). Scaling algorithms for unbalanced transport problems. *arXiv preprint: arXiv:1607.05816*.

Courty, N. (2017). Optimal transport for domain adaptation. *IEEE Transactions on Pattern Analysis and Machine Intelligence*, 39(9):1853–1865.

Cuturi, M. (2013). Sinkhorn distances: Lightspeed computation of optimal transport. In *NeurIPS*.

Dantas, C. F., Soubies, E., and Févotte, C. (2021). Safe screening for sparse regression with the Kullback-Leibler divergence. In *ICASSP*.

Efron, B., Hastie, T., Johnstone, I., and Tibshirani, R. (2004). Least angle regression. *Annals of Statistics*, 32:407–489.

Ghaoui, L. E., Viallon, V., and Rabbani, T. (2010). Safe feature elimination for the lasso and sparse supervised learning problems. *arXiv preprint arXiv:1009.4219*.

Janati, H., Cuturi, M., and Gramfort, A. (2019). Wasserstein regularization for sparse multi-task regression. In *AISTATS*.

Kantorovich, L. (1942). On the transfer of masses. *Dokl. Akad. Nauk*, 37(2):227–229.

Lee, D. D. and Seung, H. S. (2000). Algorithms for non-negative matrix factorization. In *NIPS*.

Liero, M., Mielke, A., and Savaré, G. (2018). Optimal entropy-transport problems and a new hellinger–kantorovich distance between positive measures. *Inventiones mathematicae*, 211(3):969–1117.

Liu, J., Zhao, Z., Wang, J., and Ye, J. (2014). Safe screening with variational inequalities and its application to lasso. In *ICML*.

Maretic, H. P., Gheche, M. E., Chierchia, G., and Frossard, P. (2019). GOT: An optimal transport framework for graph comparison. In *NeurIPS*.

Ndiaye, E., Fercoq, O., Alex, re Gramfort, and Salmon, J. (2017). Gap safe screening rules for sparsity enforcing penalties. *Journal of Machine Learning Research*, 18(128):1–33.

Nguyen, Q. M., Nguyen, H. H., Zhou, Y., and Nguyen, L. M. (2022). On unbalanced optimal transport: Gradient methods, sparsity and approximation error. *arXiv preprint arXiv:2202.03618*.

Ogawa, K., Suzuki, Y., and Takeuchi, I. (2013). Safe screening of non-support vectors in pathwise SVM computation. In *ICML*.

Pham, K., Le, K., Ho, N., Pham, T., and Bui, H. (2020). On unbalanced optimal transport: An analysis of Sinkhorn algorithm. In *ICML*.

Rockafellar, R. T. and Wets, R. J. B. (1998). *Variational Analysis*. Springer.

Schiebinger, G., Shu, J., Tabaka, M., Cleary, B., Subramanian, V., Solomon, A., Gould, J., Liu, S., Lin, S., Berube, P., Lee, L., Chen, J., Brumbaugh, J., Rigollet, P., Hochedlinger, K., Jaenisch, R., Regev, A., and Lander, E. S. (2019). Optimal-transport analysis of single-cell gene expression identifies developmental trajectories in reprogramming. *Cell*, 176(4):928–943.e22.

Schmitzer, B. (2016). Stabilized sparse scaling algorithms for entropy regularized transport problems. *CoRR*, abs/1610.06519.

Sinkhorn, R. (1974). Diagonal equivalence to matrices with prescribed row and column sums. ii. *Proceedings of the American Mathematical Society*, 45(2):195–198.

Tibshirani, R. (1996). Regression shrinkage and selection via the lasso. *Journal of the Royal Statistical Society. Series B (Methodological)*, 58(1):267–288.

Villani, C. (2008). *Optimal Transport: Old And New.* Springer.

Wang, J., Wonka, P., and Ye, J. (2015). Lasso screening rules via dual polytope projection. *Journal of Machine Learning Research*, 16:1063–1101.

Xiang, Z. J., Wang, Y., and Ramadge, P. J. (2017). Screening tests for lasso problems. *IEEE Transac-*

tions on Pattern Analysis and Machine Intelligence, 39(5):1008–1027.

Yamada, H. and Yamada, M. (2021). Dynamic sasvi: Strong safe screening for norm-regularized least squares. In *NeurIPS*.

Yang, K. D. and Uhler, C. (2019). Scalable unbalanced optimal transport using generative adversarial networks. In *ICLR*.

Supplementary Material:
Safe Screening for ℓ_2-norm Penalized Unbalanced Optimal Transport

A PROOFS

A.1 Proof of Theorem 5

From the (Yamada and Yamada, 2021, Proposition 3) we know that:

$$\mathbf{X}\hat{\boldsymbol{t}} \in \partial h^*(-\hat{\boldsymbol{\theta}}) \wedge \hat{\boldsymbol{t}} \in \partial g^*(\mathbf{X}^T\hat{\boldsymbol{\theta}}) \tag{15}$$

where ∂ is the subgradient, then we know that $\mathbf{X}^T\hat{\boldsymbol{\theta}} \in \partial g(\hat{\boldsymbol{t}})$, compute and you can get the **Theorem 5**.

A.2 Proof of Theorem 7

For any $p \in 0, 1, ..., nm-1$, then we can compute that:

$$
\begin{aligned}
\boldsymbol{x}_p^T\tilde{\boldsymbol{\theta}} &= \tilde{\boldsymbol{\alpha}}_u + \tilde{\boldsymbol{\beta}}_v \\
&= \boldsymbol{\alpha}_u + \boldsymbol{\beta}_v - \max_{0 \le j < n} \frac{\boldsymbol{\alpha}_u + \boldsymbol{\beta}_j - \lambda \boldsymbol{c}_{un+j}}{2} - \max_{0 \le i < m} \frac{\boldsymbol{\alpha}_i + \boldsymbol{\beta}_v - \lambda \boldsymbol{c}_{in+v}}{2} \\
&\le \boldsymbol{\alpha}_u + \boldsymbol{\beta}_v - \frac{\boldsymbol{\alpha}_u + \boldsymbol{\beta}_v - \lambda \boldsymbol{c}_p}{2} - \frac{\boldsymbol{\alpha}_u + \boldsymbol{\beta}_v - \lambda \boldsymbol{c}_p}{2} \\
&\le \lambda \boldsymbol{c}_p
\end{aligned} \tag{16}
$$

For $\forall p$, we have $\tilde{\boldsymbol{\theta}} \in \mathcal{R}^D$

A.3 Proof of Theorem 6

We Generalize the problem as

$$\max_{\boldsymbol{\theta} \in \mathcal{R}_I^S} \boldsymbol{\theta}_{I_1} + \boldsymbol{\theta}_{I_2} \tag{17}$$

Considering the center of the circle as $\boldsymbol{\theta}^o$, we define $\boldsymbol{\theta} = \boldsymbol{\theta}^o + q$, as $\boldsymbol{\theta}_{I_1}^o + \boldsymbol{\theta}_{I_2}^o$ is a constant, the problem is equal to $\min_{\boldsymbol{\theta} \in \mathcal{R}_I^S} -(\boldsymbol{q}_{I_1} + \boldsymbol{q}_{I_2})$, we compute the Lagrangrian function of later:

$$\min_{\boldsymbol{q}} \max_{\eta,\mu,\nu \ge 0} L(\boldsymbol{q}, \eta, \mu, \nu) = \min_{\boldsymbol{q}} \max_{\eta,\mu,\nu \ge 0} -\boldsymbol{q}_{I_1} - \boldsymbol{q}_{I_2} + \eta(\boldsymbol{q}^T\boldsymbol{q} - r^2) + \mu(a^T\boldsymbol{q} - e_a) + \nu(b^T\boldsymbol{q} - e_b) \tag{18}$$

$$\frac{\partial L}{\partial \boldsymbol{q}_i} = \begin{cases} -1 + 2\eta\boldsymbol{q}_i + \mu a_i + \nu b_i & i = I_1, I_2 \\ 2\eta\boldsymbol{q}_i + \mu a_i + \nu b_i & i \ne I_1, I_2 \end{cases} \tag{19}$$

$$\boldsymbol{q}_i^* = \begin{cases} \dfrac{1 - \mu a_i - \nu b_i}{2\eta} & i = I_1, I_2 \\ -\dfrac{\mu a_i + \nu b_i}{2\eta} & i \ne I_1, I_2 \end{cases} \tag{20}$$

We can get the Lagrangian dual problem:

$$\max_{\eta,\mu,\nu \ge 0} L(\eta, \mu, \nu) = \max_{\eta,\mu,\nu \ge 0} \frac{\mu a_{I_1} + \nu b_{I_1} - 1}{2\eta} + \frac{\mu a_{I_2} + \nu b_{I_2} - 1}{2\eta} + \eta(\boldsymbol{q}^{*T}\boldsymbol{q}^* - r^2) + \mu(a^T\boldsymbol{q}^* - e_a) + \nu(b^T\boldsymbol{q}^* - e_b) \tag{21}$$

From the KKT optimum condition, we know that if

$$
\begin{aligned}
\eta(\boldsymbol{q}^{*T}\boldsymbol{q}^* - r^2) &= 0 \\
\mu(a^T\boldsymbol{q}^* - e_a) &= 0 \\
\nu(b^T\boldsymbol{q}^* - e_b) &= 0
\end{aligned}
\tag{22}
$$

We set η^*, μ^*, ν^* as the solution of the equations, which is also the solution of the dual problem. Firstly, we assume that $\eta^*, \mu^*, \nu^* \neq 0$, then the solution is equal to compute the following equations:

$$
(1 - \mu a_{I_1} - \nu b_{I_1})^2 + (1 - \mu a_{I_2} - \nu b_{I_2})^2 + \sum_{i \neq I_1, I_2}^{m+n} (a_i\mu + b_i\nu)^2 - 4\eta^2 r^2 = 0
$$

$$
a_{I_1} - \mu a_{I_1}^2 - \nu b_{I_1}a_{I_1} + a_{I_2} - \mu a_{I_2}^2 - \nu b_{I_2}a_{I_2} - \sum_{i \neq I_1, I_2}^{m} (a_i^2\mu + b_i a_i\nu) - 2\eta e_a = 0 \tag{23}
$$

$$
b_{I_1} - \nu b_{I_1}^2 - \mu b_{I_1}a_{I_1} + b_{I_2} - \nu b_{I_2}^2 - \mu b_{I_2}a_{I_2} - \sum_{i \neq I_1, I_2}^{m} (b_i^2\nu + b_i a_i\mu) - 2\eta e_b = 0
$$

Rearranged as:

$$
\begin{aligned}
2 - 2\mu(a_{I_1} + a_{I_2}) - 2\nu(b_{I_1} + b_{I_2}) + \|a\|^2\mu^2 + \|b\|^2\nu^2 + 2\mu\nu a^T b - 4\eta^2 r^2 &= 0 \\
(a_{I_1} + a_{I_1}) - \|a\|^2\mu - a^T b\nu - 2\eta e_a &= 0 \\
(b_{I_1} + b_{I_2}) - \|b\|^2\nu - a^T b\mu - 2\eta e_b &= 0
\end{aligned}
\tag{24}
$$

we have

$$
\begin{aligned}
\mu &= \frac{2(e_b a^T b - e_a\|b\|^2)\eta + (a_{I_1} + a_{I_2})\|b\|^2 - (b_{I_1} + b_{I_2})(a^T b)}{\|a\|^2\|b\|^2 - a^T b} \\
\nu &= \frac{2(e_a a^T b - e_b\|a\|^2)\eta + (b_{I_1} + b_{I_2})\|a\|^2 - (a_{I_1} + a_{I_2})(a^T b)}{\|a\|^2\|b\|^2 - a^T b}
\end{aligned}
\tag{25}
$$

set it as:

$$
\begin{aligned}
\mu &= s_1\eta + s_2 \\
\nu &= u_1\eta + u_2
\end{aligned}
\tag{26}
$$

Then we can solve the η as a quadratic equation:

$$
\begin{aligned}
0 &= a\eta^2 + b\eta + c \\
a &= 4r^2 - s_1^2\|a\|^2 - u_1^2\|b\|^2 - 2s_1 u_1 a^T b \\
b &= 2(a_{I_1} + a_{I_2})s_1 + 2(b_{I_1} + b_{I_2})u_1 - 2s_1 s_2\|a\|^2 - 2u_1 u_2\|b\|^2 - 2(s_1 u_2 + s_2 u_1)a^T b \\
c &= 2(a_{I_1} + a_{I_2})s_2 + 2(b_{I_1} + b_{I_2})u_2 - s_2^2\|a\|_1 - u_2^2\|b\|_1 - 2s_2 u_2 a^T b - 2
\end{aligned}
\tag{27}
$$

Then we can put it back into 26 and get μ, ν.

If the solution satisfied the constraints $\eta^*, \mu^*, \nu^* > 0$, then it is the solution. However, if one of the dual variables is less than 0, the problem would degenerate into a simpler question.

If only η^* is larger than 0, $\min_{\boldsymbol{\theta} \in \mathcal{R}_I^S} -(\boldsymbol{q}_{I_1} + \boldsymbol{q}_{I_2}) = -\sqrt{2}r$

If only μ^* or ν^* is less than 0, we are optimizing on a sphere cap, the solution can be found in (Yamada and Yamada, 2021, supplementary material B)

if only $\eta^* \leq 0$: As the sphere is inactivated, the problem gets maximum at every point of the intersection of two planes.

$$
\min_{\boldsymbol{q}} \max_{\mu, \nu \geq 0} L(\boldsymbol{q}, \mu, \nu) = \min_{\boldsymbol{q}} \max_{\mu, \nu \geq 0} -\boldsymbol{q}_{I_1} - \boldsymbol{q}_{I_2} + \mu(a^T\boldsymbol{q} - e_a) + \nu(b^T\boldsymbol{q} - e_b)
\tag{28}
$$

To have a solution, the equations satisfied

$$\frac{\partial L}{\partial q} = \begin{cases} -1 + \mu a_i + \nu b_i = 0 & i = I_1, I_2 \\ -\mu a_i - \nu b_i & = 0 \, i \neq I_1, I_2 \end{cases} \tag{29}$$

As the equation satisfied, we can just set $\boldsymbol{q}_i^* = 0, i \neq I_1, I_2$, then we compute the

$$\min_{\boldsymbol{\theta} \in \mathcal{R}_I^S} -(\boldsymbol{q}_{I_1} + \boldsymbol{q}_{I_2}) = \frac{a_{I_2} e_b - b_{I_2} e_a - a_{I_1} e_b + b_{I_1} e_a}{a_{I_1} b_{I_2} - a_{I_2} b_{I_1}} \tag{30}$$